Conformation of the C-Terminal Domain of the Pro-Apoptotic Protein Bax and Mutants and Its Interaction with Membranes†

María del Mar Martínez-Senac, Senena Corbalán-García, and Juan C. Gómez-Fernández*

Departamento de Bioquímica y Biología Molecular-A, Edificio de Veterinaria, Universidad de Murcia, Apartado de Correos 4021, E-30080-Murcia, Spain

Received April 3, 2001; Revised Manuscript Received June 18, 2001

ABSTRACT: The C-terminal domain of the pro-apoptotic protein Bax is a hydrophobic stretch which, it has been predicted, anchors this protein to the outer mitochondrial membrane when apoptosis is induced in the cell. A 21mer peptide imitating this domain has been synthesized together with two mutants, one with a S184 substituted by K and the other with the S184 deleted. When their structures were studied by infrared spectroscopy, it was seen that the three peptides formed aggregates both in solution and within lipid membranes, and that the peptide changed its secondary structure as a consequence of these two mutations. It was also observed that the wild-type peptide and the two mutants became membrane-integral molecules and changed their conformation when they were incorporated into model membranes with the same composition as the outer mitochondrial membrane. With the peptides incorporated in the membranes the location of W188 was studied by fluorescence quenching using the water soluble quencher acrylamide and different doxyl-PC located in the membrane, this residue being found at different membrane depths in each of the three peptides. The fact that the three peptides were able to perturb the motion of the fluorescent probe diphenylhexatriene confirmed their insertion in the membrane. However, whereas the wild type and the ΔS184 mutant peptides were very efficient in releasing encapsulated carboxyfluorescein from liposomes, the mutant S184K was less efficient. Taken together, these results showed that the mutation tested changed the conformation of the C-terminal domain of Bax and the positions that they adopted when inserted in membranes, confirming the importance of S184 determining the conformation of this domain. At the same time, these results confirmed that the C-terminal domain of Bax participates in disrupting the barrier properties of biomembranes.

Apoptosis is a highly ordered and controlled program of cell death that controls normal tissue homeostasis by balancing cell proliferation and death (*1*−*3*). Among the various apoptotic factors identified, Bcl-2 family members play a key role. The Bcl-2 family is composed of both anti-apoptotic (Bcl-2, Bcl-x_L, Bcl-w, Mcl-1, A1, NR13, BHRF1, LMW5-HL, ORF16, KS-Bcl-2, ElB-19K, and CED-9) and pro-apoptotic (Bax, Bak, Bok, Bik, Blk, Hrk, BNIP3, Bim_L, Bad, Bid, and EGL-1) molecules (*4*). These proteins can form homo- and heterodimers that involve amino acid sequences known as Bcl-2 homology (BH) domains. Four of these domains, BH1 to BH4, have been identified (*5*−*8*). The ratio between pro- and anti-apoptotic proteins helps to determine, in part, the susceptibility of cells to a death signal. Proteins in the Bcl-2 family are able to form homo- and heterodimers (*9*−*11*). It is known that the BH3 domain of the pro-apoptotic members is required for anti- and pro-apoptotic members to interact (*12*).

The principal site of action of some of the Bcl-2 family members appears to be the mitochondrion (*13*−*16*). Mitochondria may trigger apoptosis by releasing among other proteins cytochrome *c* (*15*, *17*−*20*) and the apoptosis inducing factor (*21*), among others, leading to caspases activation (*22*). The mechanisms through which these proteins perform their function are as yet unknown. It seems that some members of this family are integral membrane proteins and some have been demonstrated to form ion channels in vitro (*23*−*26*).

Bax, a 21-kDa death-promoting member of the Bcl-2 family, was identified by virtue of its association with Bcl-2 (*9*). Determination of the amino acid sequence of the Bax protein showed it to be highly homologous to Bcl-2. Both proteins have three conserved regions known as BH1, BH2, and BH3 domains, and hydropathy analysis of the sequences of these proteins points to the presence of a hydrophobic transmembrane segment at their C-terminal ends.

A study of the subcellular localization of Bax has shown that it is a soluble protein predominantly present in the cytosol or as membrane-peripheral in healthy living cells that, upon induction of apoptosis, translocates into mitochondria (*27*−*29*). This translocation process is rapid and occurs at an early stage of apoptosis (*27*). It has also been observed that Bax expression triggers cytochrome *c* release from the mitochondrial intermembrane space to the cytosol (*7*). It has been observed recently that Bax is present as a high molecular weight oligomer complex in the mitochondrial membrane of apoptotic cells, and it has been suggested that

† This work was supported by Grant PB98-0389 from Dirección General de Enseñanza Superior e Investigación Científica (Madrid, Spain).

* To whom correspondence should be addressed. Telephone and Fax: 34-968364766. E-Mail: jcgomez@um.es.

10.1021/bi010667d CCC: $20.00
Published on Web 07/26/2001

these oligomers may form a channel through which cytochrome *c* and other mitochondrial proteins are released to the cytosol, thus triggering apoptosis (*30*).

The solution structure of Bax has recently been determined through NMR spectroscopy (*31*) by which means it was seen to consist of nine α-helices, one of which corresponds to the C-terminal domain and occupying the hydrophobic pocket proposed previously to mediate heterodimer formation and the bioactivity of opposing members of the Bcl-2 family. The structure shows that the orientation of the C-terminal domain provides simultaneous control over its mitochondrial targeting and dimer formation.

The 21-amino acid C-terminal hydrophobic segment of Bax appears to play a role in directing Bax to mitochondria during apoptosis, as deletion of this segment in Bax abrogates its ability to insert itself into mitochondria during this process (*27*). It has been described that insertion into the membrane of Bax is somehow inhibited by its N-terminal domain (*29*, *32*), and it has been shown that both full-length Bax and a truncated form (which lacks the C-terminal domain) may destabilize model membranes, while the full-length form has increased potency (*33*). Furthermore, substitution of the C-terminus of Bax by that of Bcl-x_L does not affect its subcellular localization but abrogates its pro-apoptotic properties (*34*). The conformation of the Bax C-terminal domain has been shown to regulate subcellular location and cell death (*35*). Specifically, S184 was found to be the most important residue in determining Bax subcellular localization. In particular, wild-type Bax is located in the cytosol in healthy cells and becomes mitochondrion-bound in cells undergoing apoptosis. The mutation of S184K, on the other hand, led to a diffuse cytoplasmic localization of Bax even after the cells had received a death signal and was even able to protect cells from apoptosis. Deletion of S184, on the other hand, produced a Bax mutant, which was constitutively localized in mitochondria even in healthy cells and which was much more toxic than wild-type Bax. It seems, then, that, according to the solution structure (*31*), Bax changes its conformation after triggering of apoptosis, leading to the insertion of the C-termini into the mitochondrial membrane. Mutations at the C-termini will impede or enable the interaction of the C-terminal domain with the hydrophobic pocket, explaining previous observations (*35*).

In the present study, we have used a synthetic peptide (21mer) with the same sequence as the 172−192 C-terminal domain of Bax and two mutants with the same tail, deleting S184 in one case and substituting S184 by K in the other. When its secondary structure was studied by infrared spectroscopy and its interaction with model membranes with the same lipid composition as the outer mitochondrial membrane, it was found that they inserted themselves into the membrane in a different way. This was confirmed by their unequal capacity to disturb the physical properties of the phospholipid bilayer, as seen through the release of encapsulated carboxyfluorescein and by biophysical techniques, such as the quenching of fluorescence of Trp and fluorescence polarization of the membrane probe DPH.

EXPERIMENTAL PROCEDURES

Materials. Three synthetic peptides were used, one (C-Bax) encompassing residues 172−192 of Bax ($^{+}$HN-^{172}TVTIFVAGVLTASLTIWKKMG^{192}-COO^{-}) and two different mutants, in one S184 was replaced by K184 (C-BaxS184K) and from the other S184 was deleted (C-BaxΔS184). The three peptides were obtained from Genemed (San Francisco, USA), and judged pure (>95%) according to HPLC and MALDITOF spectroscopy. Egg yolk phosphatidylcholine (EYPC),[1] 1-palmitoyl-2-oleyl-*sn*-glycero-3-phosphatidylethanolamine (POPE), cardiolipin (CL), and the nitroxide spin probes 1-palmitoyl-2-stearoyl-(5-doxyl)-*sn*-glycero-3-phosphocholine (5-doxyl-PC), 1-palmitoyl-2-stearoyl-(12-doxyl)-*sn*-glycero-3-phosphocholine (12-doxyl-PC), and 1-palmitoyl-2-stearoyl-(16-doxyl)-*sn*-glycero-3-phosphocholine (16-doxyl-PC) were obtained from Avanti Polar Lipids (Alabaster, Alabama). Phosphatidylglycerol (PG), sphingomyelin (SM), cholesterol (Chol), deuterium oxide (D_2O), 1,6-diphenyl-1,3,5-hexatriene (DPH), and 2,2,2-trifluoroethanol (TFE) were purchased from Sigma Chemicals Co. (Madrid, Spain). Phosphatidylinositol (PI) was obtained from Lipid Products (Nutfield, Surrey, U.K.). 1,2-Dipalmitoyl-L-3-phosphatidyl[*N-methyl*-^{3}H]choline (^{3}H-PC) were from Dupont (Boston, MA; specific activity of 56 Ci/mmol). All other chemicals were of analytical grade and obtained from Merck (Darmstadt, Germany).

Binding of Peptides to MLVs. The molar lipid composition of the model membranes used was designed to be the same as that of the outer mitochondrial membrane (*36*): 45% PC, 21% PE, 13% PI, 3.5% PG, 3% CL, 4.5% SM, and 10% of Chol (molar percentages). Lipids were dissolved in chloroform/methanol (1:1, v/v) in the absence or in the presence of C-Bax or Bax mutants, which when present gave a peptide/phospholipid molar ratio of 0.02. Mixtures were dried under a stream of N_2, free of O_2, and the last traces of solvents were removed by a further 3 h evaporation under high vacuum. Then, 200 μL of TFE were added and the mixture was vortexed vigorously, dried under a stream of nitrogen, and stored under vacuum for 3 h to totally remove the organic solvent. Dried samples were then hydrated in 100 μL of D_2O buffer (10 mM Hepes, pD 7.4, 0.1 mM EDTA) and dispersed with vigorous vortex mixing to form multilamellar vesicles (MLV). Note that, given the unsaturated nature of most of the acyl chains of the phospholipid used, the mixture is in fluid state at room temperature. The samples were then centrifuged at 13200*g* for 25 min.

In this way, lipid membranes were floated to give a floated phase, which was recovered from the top of the tube with the supernatant and separated from a sediment of aggregated and unincorporated peptide. The floated phase plus the supernatant were centrifuged again at 13200*g* for 25 min to obtain good separation of the membranes, which were recovered again as a floated phase. Then, to check if the peptide was incorporated into the multilamellar lipid vesicles, Trp fluorescence emission at 333 nm was measured. Each

[1] Abbreviations: EYPC, egg yolk phosphatidylcholine; POPE, 1-palmitoyl-2-oleyl-*sn*-glycero-3-phosphatidylethanolamine; CL, cardiolipin; 5-doxyl PC, 1-palmitoyl-2-stearoyl-(5-doxyl)-*sn*-glycero-3-phosphocholine; 12-doxyl PC, 1-palmitoyl-2-stearoyl-(12-doxyl)-*sn*-glycero-3-phosphocholine; 16-doxyl PC, 1-palmitoyl-2-stearoyl-(16-doxyl)-*sn*-glycero-3-phosphocholine; PG, phosphatidylglycerol; SM, sphingomielin; Chol, cholesterol; PI, phosphatidylinositol; ^{3}H-PC, 1,2-dipalmitoyl-L-3-phosphatidyl[*N-methyl*-^{3}H]choline; CF, 5(6)-carboxyfluorescein; D_2O, deuterium oxide; DPH, 1,6-diphenyl-1,3,5-hexatriene; TFE, 2,2,2-trifluoroethanol; FT-IR, Fourier transform infrared spectroscopy; MLV, multilamellar vesicles; LUV, large unilamellar vesicles.

assay mixture contained an aliquot of the membrane floated phase added to 2 mL of 20 mM Tris, pH 7.4, 100 mM NaCl, 0.5 mM EGTA, 1% SDS buffer. Trp fluorescence emission was monitored using a F-4500 HITACHI spectrofluorimeter with excitation at 295 nm (5-nm slit width) and emission wavelength scan from 300 to 450 nm (15-nm slit width). The same spectrofluorimeter was used in all the fluorescence experiments reported in this paper. Measurements were performed at 25 °C. According to these measurements, 84.5 ± 11% of C-Bax, 65.8 ± 12% of C-Bax-S184K, and 70.5 ± 14% of C-Bax-ΔS184K were incorporated to lipid membranes.

Infrared Spectroscopy. The infrared measurements were performed on a Bruker Vector 22 Fourier transform infrared spectrometer equipped with a MCT detector. Each spectrum was obtained by collecting 500 interferograms with a nominal resolution of 4 cm^{-1} and triangular apodization, using the sample shuttle accessory to average background spectra over the same time period. The spectrometer was continuously purged with dry air. Samples containing peptides plus lipids were prepared as for the binding assays, at a peptide/lipid molar ratio of 0.02, then 25 μL of membranes (recovered as floated phase from the top of the centrifuge tubes) were transferred to a Specac 20710 cell equipped with CaF_2 windows and 25-μm Teflon spacers (Specac, Kent, UK). Samples containing peptide only and no lipid were hydrated in 25 μL of D_2O buffer (10 mM Hepes, pD 7.4, 0.1 mM EDTA) and vortexed. Next, samples were transferred to the infrared cell described above. Spectral subtraction was performed interactively using the Grams-32 program (Galactic Industries Corp., Salem, NH). Data treatment and band decomposition of the original amide I′ have been described previously (*37*, *38*). The position of each individual band was obtained from the resolution-enhanced spectrum. The fractional areas of bands in the amide I′ region were calculated from the final fitted band areas.

Quenching by Acrylamide. Acrylamide quenching experiments were carried out essentially as described (*39*). Samples were prepared as described above for binding experiments and for infrared spectroscopy, except that the buffer used to hydrate samples also contained acrylamide. Different samples were prepared containing from 0 to 0.8 M acrylamide. Prior to the quenching experiments, peptide binding to liposomes was determined, as described above, by monitoring Trp fluorescence. An aliquot of the membrane floated phase was added to the mixture assay which contained 1.8 mL of 10 mM Hepes, pH 7.4, 0.1 mM EDTA buffer and different concentrations of acrylamide ranging from 0 to 0.8 M.

For experiments without lipid membranes, peptide samples were hydrated with 50 μL of D_2O buffer (10 mM Hepes, pD 7.4, 0.1 mM EDTA) and vortexed. Then, they were centrifuged at 13200*g* for 25 min, and the supernatant containing dissolved peptide was collected. The mixture assay contained dissolved peptide in 1.8 mL of buffer (10 mM Hepes, pH 7.4, 0.1 mM EDTA) and increasing concentrations of acrylamide.

Trp fluorescence emission was monitored with excitation at 295 nm (5-nm slit width) and emission intensity from 300 to 450 nm (15-nm slit width). Measurements were performed at 25 °C. The fluorescence intensity of the sample without peptide was subtracted in all cases and the inner filter effect was corrected as described (*39*).

Quenching kinetic parameters were calculated from a Stern−Volmer equation (*45*),

$$F_0/F = 1 + K_{sv}[Q]$$

where F_0 and F are the fluorescence intensity in the absence and presence of the quencher (Q), K_{sv} is a quenching constant (which is the product of the collisional quenching rate constant and fluorescence lifetime in the absence of the quencher) and [Q] is the quencher concentration.

Quenching by Doxyl-PC. A lipid mixture was prepared containing 21% PE, 13% PI, 3.5% PG, 3% CL, 4.5% SM, and 10% Chol (molar percentages) and different amounts of 5-, 12-, and 16-doxyl PCs and PC to reach 45%. As tracer, [^{3}H]-PC at a concentration of approximately 900 cpm/nmol was included in the lipid mixtures. These mixtures in the absence or in the presence of C-Bax or one of the two C-Bax mutants were dissolved in chloroform/methanol (1:1, v/v), at a peptide/phospholipid molar ratio of 0.02, dried under a stream of nitrogen, and stored under vacuum for 3 h to totally remove the organic solvent totally. Then, 200 μL of TFE was added and vortexed vigorously, and the sample was dried under a stream of N_2. Any traces of organic solvent were removed by a further 3 h evaporation under high vacuum. Samples were then prepared as described for the binding experiments. The total lipid content was quantified by liquid scintillation counting after and before centrifugation. Peptide binding to liposomes was also determined as described in the previous section.

The assay mixture contained, in a total volume of 1.8 mL, membranes obtained by floating after centrifugation, in the absence or in the presence of bound peptide and 10 mM Hepes, pH 7.4, 0.1 mM EDTA buffer. Trp fluorescence emission was monitored with excitation at 280 nm (5-nm slit width) and emission intensity from 300 to 450 nm (15-nm slit width). Measurements were performed at 25 °C. The fluorescence intensity of samples without peptide was subtracted in all cases.

Quenching kinetic parameters were calculated from a Stern−Volmer equation (*45*), as described for quenching by acrylamide experiments.

Leakage of Liposome Contents. The leakage of liposome contents to the external medium was kinetically monitored by measuring the release of the 5(6)-carboxyfluorescein (CF) trapped inside the vesicles (*40*−*43*). Since the fluorescent dye, CF, was obtained from Kodak (Eastman Kodak Co.) and contained hydrophobic impurities it was purified by gel filtration on a Sephadex LH-20 (Pharmacia) (1 × 30) column. The concentration of CF was determined by ultraviolet spectroscopy using an absorption coefficient of 70 000 M^{-1} cm^{-1} at 493 nm. The dye solution was stored at 4 °C in the dark.

To prepare large unilamellar vesicles (LUV) with a diameter of 100 nm, we used the extrusion technique (*44*). A total of 10 μmol of lipid mixture containing 45% PC, 21% PE, 13% PI, 3.5% PG, 3% CL, 4.5% SM, and 10% Chol (molar percentages) were dissolved in chloroform/methanol (1:1). As tracer, [^{3}H]-PC at a concentration of approximately 900 cpm/nmol was included. Then, the lipid mixture was dried under a stream of N_2, free of O_2. The last traces of solvents were removed by a further 3 h evaporation under high vacuum. Lipid was then hydrated in a 50 mM Mes, pH

7.4, 50 mM K_2SO_4 buffer, containing 50 mM purified CF (*41*) and dispersed by vortexing. Then a freeze−thaw cycle was repeated five times. Subsequently, the suspension was extruded 10 times through two stacked 100 nm pore size polycarbonate membranes (Millipore Inc., Bedford, MA). The external dye was separated from the vesicles by gel filtration over a Sephadex G-25 (1 × 20) column and eluted with a 50 mM Mes, pH 7.4, 100 mM K_2SO_4 buffer. Vesicles were separated from larger particles and untrapped CF eluting in the void volume of the column. To obtain a homogeneous preparation, only the top fractions of the LUV elution peak were collected and pooled. The total lipid content was quantified by liquid scintillation counting after and before the extrusion and gel filtration. The encapsulated volume was found to be 1.13 L/mol of phospholipid.

Carboxyfluorescein at 200 mM inside the vesicles was self-quenched, but when released into the medium, for example, as by detergent solubilization of the vesicles, the diluted CF fluoresced intensely. The increase in CF fluorescence intensity was followed with excitation at 490 nm (5-nm slit width) and emission at 520 nm (15-nm slit width). Measurements were made in a thermostated 2.5-mL quartz cuvette with constant stirring at room temperature (25 °C). A small volume of vesicles was diluted in the buffer (50 mM Mes, pH 7.4, 100 mM K_2SO_4) to yield 2 mL total volume at a phospholipid final concentration of 20 μM. A baseline measurement of the vesicle fluorescence alone was made for 10 min. In our experimental conditions, the spontaneous leakage rate was less than 5%. Then, Bax C-terminal peptide or Bax mutants, dissolved in TFE at 2 or 0.5 mg/mL, or TFE vehicle was added. Fluorescence was measured for 15 min, and then a small volume of concentrated Triton X-100 (0.5% final, w/v) was added to determine the maximum fluorescence attainable under conditions of totally solubilized vesicles. The addition of 3.4 μL of TFE did not produce any important leakage. The percentage of carboxyfluorescein released was determined by the following equation: $[(F_{t=15\ min} - F_0)/(F_{max} - F_0)] \times 100$, where $F_{t=15\ min}$ is the maximum intensity 15 min after addition of peptide or TFE, F_0 is the intensity of vesicles alone at time zero, and F_{max} is the intensity after addition of Triton X-100.

Fluorescence Polarization. The fluorescent probe 1,6-diphenyl-1,3,5-hexatriene (DPH) was prepared in tetrahydrofuran and its concentration was determined by UV spectroscopy using an absorption coefficient of 88 000 M^{-1} cm^{-1} at 452 nm in methanol.

To prepare multilamellar vesicles, lipid mixtures containing 45% PC, 21% PE, 13% PI, 3.5% PG, 3% CL, 4.5% SM, and 10% Chol (molar percentages) were prepared with appropriate amounts of C-Bax or C-Bax mutants, and dissolved in chloroform/methanol (1:1, v/v) to give the different peptide/phospholipid molar ratios studied. DPH was added to the organic solvent solution, before drying, to give a probe/lipid molar ratio of 1:500. Then, samples were dried under a stream of N_2, free of O_2, and the last traces of solvents were removed by a further 3 h evaporation under high vacuum. Then, 100 μL of TFE was added and vortexed vigorously, and the mixture was dried under a stream of nitrogen and stored under vacuum for 3 h to totally remove the organic solvent totally. Samples containing the lipid mixture and peptide were then hydrated in 70 μL of filtered buffer (10 mM Hepes, pD 7.4, 0.1 mM EDTA) and dispersed with vigorous vortexing in the liquid−crystalline phase to form multilamellar vesicles (MLV).

DPH fluorescence polarization was measured with excitation and emission wavelengths of 350 and 452 nm, respectively, with an excitation and emission slit width of 5 nm. Cuvette temperature was monitored continuously by means of a thermistor probe. Fluorescence polarization was measured at a constant temperature of 25 °C. A small magnetic stirring bar in the cuvette prevented settling of the vesicles.

In the fluorescence polarization experiment, the sample was excited with a polarized beam, and the components of the emission parallel or perpendicular to the direction of the excitation beam were measured. The polarization of the emitted fluorescence, P, was determined as

$$P = \frac{1 - \left(\frac{I_{90,0}}{I_{90,90}} * \frac{I_{0,90}}{I_{0,0}}\right)}{1 + \left(\frac{I_{90,0}}{I_{90,90}} * \frac{I_{0,90}}{I_{0,0}}\right)}$$

where a correction factor for the instrumental response of the two components of the emission has been applied (*45*). $I_{i,j}$, $I_{j,i}$, $I_{i,i}$, and $I_{j,j}$ indicate the fluorescence intensity when the excitation side and emission side polarizers are set at i degree (0°) and j degree (90°), respectively.

To ensure that there was no polarization due to light scattering, polarization was measured before and after sample dilution. In cases when dilution led to an increased level of P, the samples were diluted until the value of P remained constant.

RESULTS

Infrared Spectroscopy Studies of the Secondary Structure of the Peptides. The secondary structure of the 21mer peptide which imitates the C-terminal domain of Bax, encompassing residues 172−192 (C-Bax) was studied by using infrared spectroscopy and comparing it with two other peptides, in whose sequences a point mutation was introduced: S184K (C-BaxS184K) and another one in which S184 had been deleted (C-BaxΔS184). All these peptides were studied in two states: free in D_2O buffer solution and incorporated into model membranes imitating the lipid composition of the outer mitochondrial membrane, at a peptide/lipid molar ratio of 0.02. This lipid composition was chosen because Bax has been described to incorporate into outer mitochondrial membranes in the cell (*27*−*29*).

Figure 1 shows the amide I′ region of the infrared spectrum from C-Bax. When the peptide was in solution (Figure 1A), the amide I′ band was decomposed and the number and initial position of the component bands were obtained from band-narrowed spectra by Fourier deconvolution and derivation. The corresponding parameters, band position, percentage area, bandwidth of each spectral component, and assignment are shown in Table 1. It can be seen that the spectrum exhibited four components, which can be assigned to vibrations coming from peptidyl bonds and hence used to estimate the secondary structure of the peptide. The main component was centered at 1622 cm^{-1} and represented 44% of the total area, which can be assigned to β-pleated sheets and, specifically, to peptide molecules with intra- or intermolecular hydrogen bonding (*46*, *47*); such a feature is

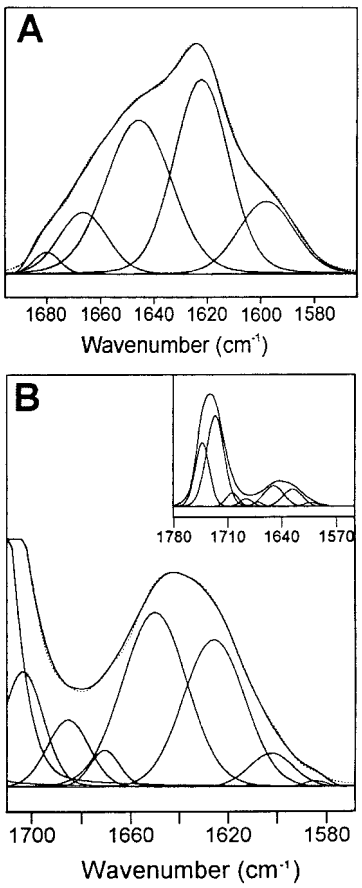

FIGURE 1: FT-IR spectrum of the Bax C-terminal domain in the absence (A) and in the presence (B) of multilamellar vesicles containing lipid mixture (45% PC, 21% PE, 13% PI, 3.5% PG, 3% CL, 4.5% SM, and 10% of Chol), at a peptide/phospholipid molar ratio of 0.02 in all the cases, in D_2O buffer with the fitted component bands. The position of the individual band was obtained from the resolution-enhanced spectrum. The parameters corresponding to the component bands are reflected in Table 1. The dotted line represents the curve-fitted spectrum.

usually found in thermally denatured proteins in D_2O buffer (*48*) and in aggregated peptides (*49*). The second most important component was centered at 1645 cm^{-1} (42%). Although this frequency is usually attributed to a random structure when observed in proteins in the presence of D_2O (*50*), in the case of peptides with highly solvent-exposed helices in D_2O, the amide I′ can shift to a frequency as low as 1644 cm^{-1} (*51*, *52*). Another component was located at 1666 cm^{-1} (12%) and the last at 1680 cm^{-1} (2%), both of which can be assigned to turns (*49*, *53*−*56*). When C-Bax was studied in the presence of membranes, four components attributable to peptidyl bonds were also obtained after band fitting of the amide I′ band (Figure 1B). The main change with respect to the peptide in solution was that the main component was now centered at 1651 cm^{-1}, representing 47% of the total area, which in D_2O buffer, can clearly be attributed to α-helix (*50*, *57*). Another component, corresponding to 37% of the total area and located at 1626 cm^{-1}, was assigned to hydrogen-bonded β-sheets, as explained above for the peptides in solution, and corresponding to 37% of the total area. The two other components centered at 1671 and 1686 cm^{-1} amounted to 5 and 11%, respectively, and both could be assigned to turns (*49*, *53*−*56*). In summary, incorporation of the peptide in the membrane resulted in an increase in the percentage of α-helical structure and a decrease in the hydrogen-bonded extended structure, whereas the percentage of turns remained similar. Membrane incorporation was also accompanied by a shift in the α-helical component of about 6 cm^{-1}, which may reflect a small reorganization in the conformation or a change in the accessibility of the α-helical structure upon insertion into the membrane (*38*). Another possibility is that the component at 1645 cm^{-1} which appeared in the spectrum in solution corresponded totally or partially to an unordered structure and that these unstructured stretches change to α-helix upon incorporation into the membrane, with a corresponding shift in vibration to 1651 cm^{-1}.

Figure 2A shows that the mutation S184K (C-BaxS184K) changed in the secondary structure of the peptide in solution. In this case, one component was located at 1624 cm^{-1} (50%), which was assigned to hydrogen-bonded β-sheet as above, one at 1645 cm^{-1} (31%) which may correspond to α-helix or α-helix plus random, and, as discussed above, two more at 1664 and 1680 cm^{-1} (11 and 8%, respectively), which were assigned to turns, according to the references given

Table 1: FT-IR Parameters of the Amide I′ Band Components of the Bax C-Terminal Domain and Mutants in the Absence or Presence of Multilamellar Vesicles Containing 45% PC, 21% PE, 13% PI, 3.5% PG, 3% CL, 4.5% SM, and 10% of Chol in 10 mM Hepes and 0.1 mM EDTA-D_2O Buffer (pD 7.4)

position[a] (cm^{-1})	assignment	area[b] (%)	position[a] (cm^{-1})	assignment	area[b] (%)
	C-Bax			C-Bax + model membranes	
1680	turns	2	1686	turns	11
1666	turns	12	1671	turns	5
1645	α-helix + random	42	1651	α-helix	47
1622	hydrogen-bonded β-sheet	44	1626	hydrogen-bonded β-sheet	37
	C-BaxS184K			C-BaxS184K + model membranes	
1680	turns	8	1684	turns	7
1664	turns	11	1671	turns	11
1645	α-helix + random	31	1649	α-helix	36
1624	hydrogen-bonded β-sheet	50	1626	hydrogen-bonded β-sheet	45
	C-BaxΔS184			C-BaxΔS184 + model membranes	
1679	turns	10	1685	turns	14
1664	turns	5	1668	turns	14
1648	α-helix	34	1648	α-helix	38
1623	hydrogen-bonded β-sheet	51	1625	hydrogen-bonded β-sheet	34

[a] Peak position of the amide I′ band components. [b] Percentage area of the band components of amide I′. The areas corresponding to side chain contributions located at 1615−1600 cm^{-1} have not been considered.

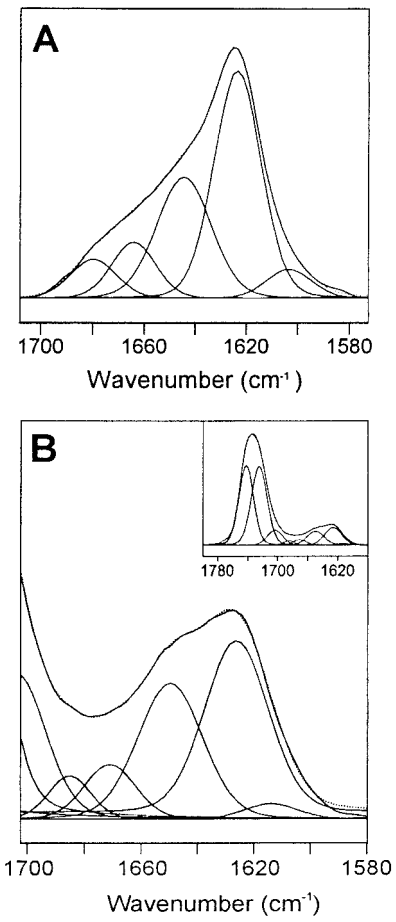

FIGURE 2: FT-IR spectrum of the mutant C-BaxS184K in the absence (A) and in the presence (B) of multilamellar vesicles containing lipid mixture (45% PC, 21% PE, 13% PI, 3.5% PG, 3% CL, 4.5% SM, and 10% of Chol), at a peptide/phospholipid molar ratio of 0.02 in all the cases, in D_2O buffer with the fitted component bands. The position of the individual band was obtained from the resolution-enhanced spectrum. The parameters corresponding to the component bands are reflected in Table 1. The dotted line represents the curve-fitted spectrum.

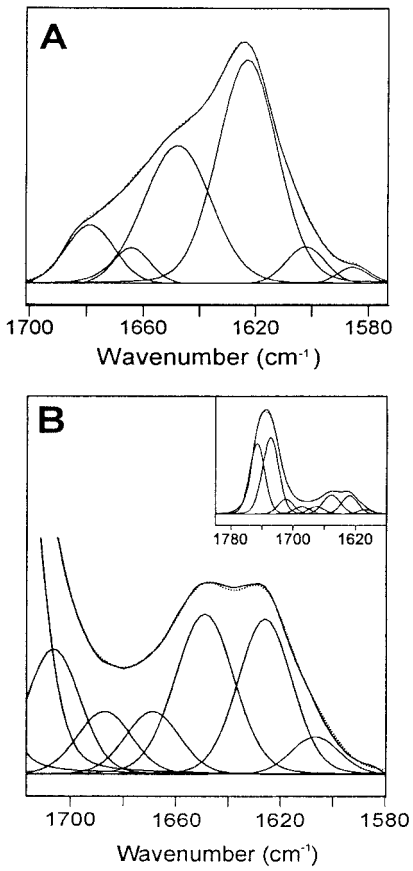

FIGURE 3: FT-IR spectrum of the C-BasΔS184 in the absence (A) and in the presence (B) of multilamellar vesicles containing lipid mixture (45% PC, 21% PE, 13% PI, 3.5% PG, 3% CL, 4.5% SM, and 10% of Chol), at a peptide/phospholipid molar ratio of 0.02 in all the cases, in D_2O buffer with the fitted component bands. The position of the individual band was obtained from the resolution-enhanced spectrum. The parameters corresponding to the component bands are reflected in Table 1. The dotted line represents the curve-fitted spectrum.

above. In the presence of membranes (Figure 2B), the main component of this peptide was that attributed to a hydrogen-bonded β-structure, appearing at 1626 cm^{-1} and representing 45% of the total area. The second was that at 1649 cm^{-1}, which amounted to 36% and corresponded to α-helix, and finally two components at 1671 and 1684 cm^{-1} which were attributed to turns (11 and 7%, respectively, of the total area). In the case of this C-BaxS184K peptide, the change observed in the secondary structure as it passed from solution into the membrane was very similar to that discussed above for C-Bax, with a certain increase in α-helix at the expense of β-sheet.

Deletion of serine-184 produced a peptide (C-BaxΔS184) which, after band fitting, showed components at the same frequencies as those of the peptides presented above. Therefore, the same references apply and will be omitted for the sake of brevity. C-BaxΔS184 in solution showed components (Figure 3A) at 1623 cm^{-1}, attributed to hydrogen-bonded β-sheet and corresponding to 51% of the total area, at 1648 cm^{-1} (34%) corresponding to α-helix, and at 1664 and 1679 cm^{-1} (5 and 10%, respectively) assigned to turns. In the presence of membranes (Figure 3B) band-fitting of the amide-I′ band of C-BaxΔS184 gave components at 1625 cm^{-1} (34%), attributed to hydrogen-bonded β-structure, 1648 cm^{-1} (38%), attributed to α-helix, and 1668 and 1685 cm^{-1} (14 and 14%, respectively), attributed to turns. The structure of this peptide in solution, seems to be similar to that of the other two peptides examined above. The most noticeable effect observed when C-BaxΔS184 was incorporated into membranes was the increase in the proportion represented by turns, which went up from 15% in solution to 28% in the membrane at the expense of the β-sheet component.

Location of the W188 residue using fluorescence quenching techniques. The first technique used to quench fluorescence involved the hydrophilic quencher acrylamide, which does not penetrate the membrane (*58*−*62*) and which therefore provides information on the accessibility of a membrane fluorophore to the external medium. Figure 4 shows a comparison of the quenching of the three peptides studied both in solution and in the presence of membranes. It can be seen that all three peptides are efficiently quenched in solution although K_Q is considerably higher for C-Bax (30.5 M^{-1}) than for C-BaxS184K (14.9 M^{-1}) and C-BaxΔS184 (10.4 M^{-1}), which may indicate that C-Bax adopts an inter- or intramolecular conformation, this facilitating access of the quencher. In the presence of membranes, the accessibility of the Trp residue is again considerably reduced with a K_Q of 5.8 M^{-1} for C-Bax, but only 1.1 M^{-1} for

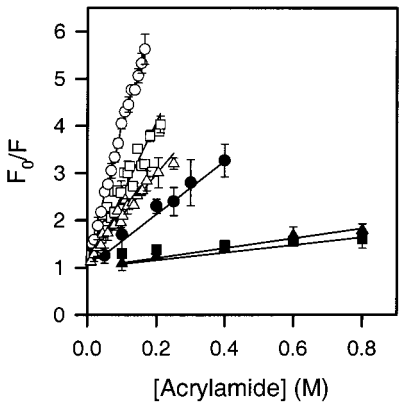

FIGURE 4: Stern−Volmer plots of the quenching of tryptophan fluorescence of the Bax C-terminal domain (circles), C-BasS184K (squares) and C-BaxΔS184 (triangles) by acrylamide. Peptide incorporated in model membranes used 45% PC, 21% PE, 13% PI, 3.5% PG, 3% CL, 4.5% SM, and 10% of Chol at a peptide/lipid molar ratio of 0.02 (black symbols) and peptides alone (in the absence of phospholipid) (white symbols). Measurements were made in triplicate.

C-BaxS184K and 1.0 M^{-1} for C-BaxΔS184. This means that when these peptides are associated with the membrane, access to this Trp is almost totally precluded for C-BaxS184K and C-BaxΔS184 and much more difficult for C-Bax.

The other approach used was to quench the fluorescence of W188 using quenchers located at carbons occupying different positions in the acyl chain of the phospholipids within the membrane. The quenchers 5-, 12-, and 16-doxyl-PC were used with the three peptides studied to assay the depth of penetration. Figure 5A shows that, in the case of C-Bax, quenching was very low for the three quenchers used. However, the slightly higher degree of quenching obtained with the 5-doxyl-PC indicated that W188 was located superficially in the membrane, which agrees well with the results of the acrylamide quenching shown above. In the case of C-BaxS184K, very efficient quenching was produced by 12-doxyl-PC, and a lower degree by 5-doxyl-PC (Figure 5B), indicating that, in this case, W188 was deeply located in the membrane, nominally between carbons 12 and 5, and closer to 12 than to 5. Finally, the quenching of C-BaxΔS184 was very efficient by 5-doxyl-PC and less so by 12-doxyl-PC, indicating that W188 is nominally closer to carbon 5 than to carbon 12, but between both of them (Figure 5C).

Fluorescence Polarization of Diphenyl Hexatriene. To further assess the penetration of the peptides in the membrane, experiments were performed in which the steady-state polarization value (Figure 6) was measured with increasing concentrations of the peptide. The results show that this value increased from 0.2 in the pure lipid to 0.3 at a peptide/lipid molar ratio of 0.3. The effect was very similar for the three peptides and similar to the effects reported for a variety of intrinsic molecules, such as Ca^{2+}-ATPase (*63*), cholesterol and cytochrome *c* oxidase (*64*), bacteriorhodopsin (*65*), myelin apolipoprotein (*66*), Pf-1 viral protein (*67*), α-haemolysin (*68*), and, more recently, with the C-terminal domain of Bcl-2 (*49*) and the C-terminal domain of Bak (*69*).

Leakage of 6-Carboxyfluorescein Induced by Bax C-Terminal Domain Peptides. To further assess the insertion of the peptides in the membranes, the release of encapsulated 5(6)-carboxyfluorescein trapped inside the vesicles was monitored at increasing concentrations of peptide. Figure 7 shows the percentages released 15 min after addition of the peptides. It can be seen that C-BaxΔS184 was the most efficient peptide in inducing the release and very closely

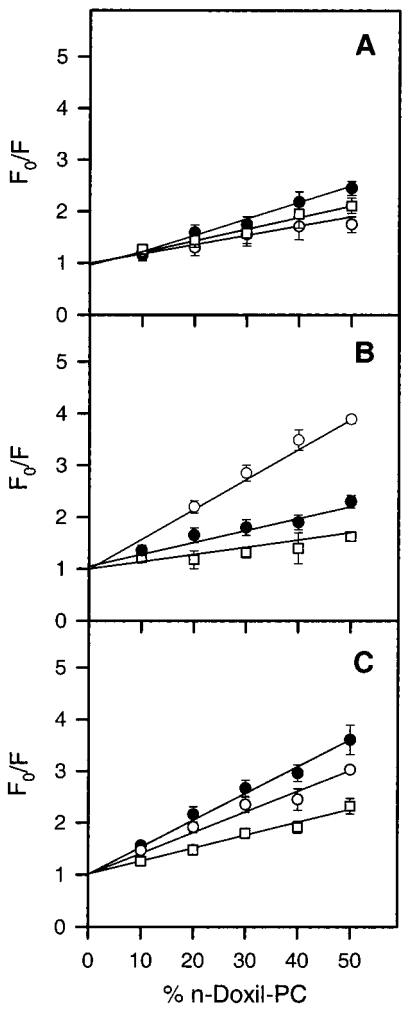

FIGURE 5: Stern−Volmer plots of the quenching of tryptophan fluorescence of the Bax C-terminal domain (A), C-BasS184K (B), and C-BaxΔS184 (C) by 5-doxyl-PC (●), 12-doxyl-PC (○), and 16-doxyl-PC (□). Peptide incorporated in model membranes used 45% PC, 21% PE, 13% PI, 3.5% PG, 3% CL, 4.5% SM and 10% of Chol at a peptide/lipid molar ratio of 0.02. Measurements were made in triplicate.

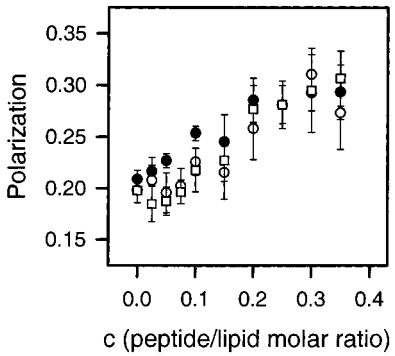

FIGURE 6: Polarization of DPH fluorescence in model membranes (45% PC, 21% PE, 13% PI, 3.5% PG, 3% CL, 4.5% SM, and 10% of Chol) (MLV) (10 μM) (probe/lipid molar ratio of 1:500) with Bax C-terminal domain (●), C-BaxS184K (○), and C-BaxΔS184 (□) at increasing molar fractions. Experiments were carried out at 25 °C and constant stirring. Measurements were made in two independent experiments with 20 determinations for each experiment.

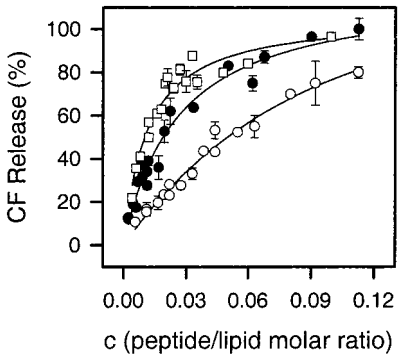

FIGURE 7: Leakage of carboxyfluorescein from model membranes (45% PC, 21% PE, 13% PI, 3.5% PG, 3% CL, 4.5% SM, and 10% of Chol) (LUV) induced by the Bax C-terminal domain (●), C-BaxS184K (○), and C-BaxΔS184 (□). The percentage of carboxyfluorescein released after 15 min of incubation with increasing concentrations of peptide was plotted as a function of the peptide/lipid molar ratio (c). 100% of leakage was established by lysing SUV with Triton X-100 (0.5%, w/v). Error bars indicate the SEM for quadruplicate determinations.

followed by C-Bax, and C-BaxS184K was less efficient. These data suggest that C-BaxΔS184 can mimic C-Bax and how, on the other hand, the substitution of the S184 to K considerably affects CF release.

DISCUSSION

We have studied the structure of the C-terminal domain of Bax and two mutants and their capacity to incorporate into model membranes. Since Bax is thought to incorporate into the outer mitochondrial membrane, we have used vesicles with the same lipid composition as this biomembrane. The results obtained using different biophysical techniques confirmed that the three peptides used were capable of incorporating into the membranes.

With respect to the secondary structure, infrared spectroscopy showed that the three peptides in solution possessed a secondary structure, where the hydrogen-bonded β-pleated sheet predominated and slightly decreased in percentage in all three cases as a consequence of their incorporation into membranes. This is somewhat similar to that described in a previous work for the C-terminal domain of Bcl-2 (*49*), or for the C-terminal domain of Bak (*69*) although these last two peptides extensively changed their structure upon insertion into membranes, showing a clear predominance of α-helix. It is very interesting that the amino acid sequences of the C-terminal domains of Bcl-2, Bak, and Bax have a certain similarity, all three sharing a hydrophobic core and a positive charge at the C-terminus. Bax and Bak, both of which are pro-apoptotic, have 80% homology in their C-terminal domains.

However, even in membranes, the Bax peptides studied here maintain a substantial percentage of hydrogen-bonded β-sheet, which is unusual for intrinsic proteins or peptides. It should be borne in mind that Bax has very recently been described as being oligomerized when free in the cytosol and also after association with mitochondria, and that such oligomerization appears to be required for its pro-apoptotic activity (*30*).

Fluorescence polarization of DPH confirmed that the three peptides were capable of perturbing the motion of the probe, this being compatible with the incorporation of all of them into the membrane.

The quenching constant (K_Q) calculated in the fluorescence quenching experiments carried out to locate the Trp residue (W188) indicated that this residue is more accessible to the hydrophilic quencher acrylamide in C-Bax than in the two mutants when they are in solution. This indicates that there is a higher exposure to medium of the Trp residue in C-Bax than in the two mutants. On the other hand, acrylamide quenching shows that the Trp fluorophore is clearly embedded in the membrane in the cases of C-BaxS184K and C-BaxΔS184. The results obtained by quenching with doxyl-PCs confirmed that W188 is not immersed deeply in the lipid bilayer in the case of C-Bax, but seems to be localized near the lipid−water interface, as can be deduced from the low quenching level observed. This is in agreement with the acrylamide quenching results, which show a limited decrease in accessibility in the membrane as compared with the peptide in solution. According to the quenching with doxyl-PCs, it seems that W188 was most deeply embedded in the membrane in the case of C-BaxS184K, where it was supposedly located nearer to C12 than to C5 of the acyl chains of phospholipids, whereas in the case of C-BaxΔS184, it was nearer C5 than C12.

The capacity of the different peptides to release CF, however, was not the same; while C-BaxΔS184 and C-Bax were quite efficient, C-BaxS184K was less efficient in releasing CF under the conditions used. The explanation for this differential behavior is presumably that C-Bax and C-BaxΔS184 are able to form pores, whereas C-BaxS184K has a lower capacity. The inclusion of a charged residue like a Lys in the middle of a hydrophobic stretch may create problems in its ability to disrupt the membrane.

Taking into account the acrylamide and doxyl-PC quenching experiments performed to locate W188, which is at the C-terminal part of the peptides, it was concluded that C-Bax leaves its fluorophore near the lipid−water interface. However, since it produces pores and perturbs the motion of DPH it must be concluded that the N-terminal part of this peptide protrudes from the membrane. C-BaxΔS184 supposedly has its W188 located near C5, and its N-terminal part probably lies deeper in the membrane. On the other hand, C-BaxS184K has its W188 located deep inside the membrane but given its low capacity to release CF, it is not clear that it would protrude the membrane.

It was previously shown (*35*) that the subcellular localization of Bax is determined by the conformation of the C-terminal tail. Mutations and the deletion of S184 can shift Bax from becoming more toxic to being death protective. In our case, these two mutations produced conformational changes in the peptides both in solution and incorporated into model membranes. Thus, the component corresponding to α-helical decreased under mutagenesis and the hydrogen-bonded β-sheet increased. This confirmed the importance of S184 in the conformation of the C-terminal domain. All these peptides, however, were capable of entering membranes in our case. Note that there is a good correlation between the biophysical and biological data.

It is interesting to note that deletion of S184 produced a peptide (C-BaxΔS184) which penetrated the membrane, and it was very efficient at releasing carboxyfluorescein. In full Bax, this mutation led indeed to its enhanced incorporation in the mitochondria. In the same way, S184K mutation (C-BaxS184K), which was not so efficient in releasing

carboxyfluorescein and which prevented full-length Bax from incorporate itself into mitochondria. However, the mutant S184K was still able of incorporating into the membrane and inducing some release of CF. The explanation for this might be that new intra- or intermolecular interactions are established by the introduction of the mutation S184K, so that although the isolated peptide is perfectly capable of incorporating itself into membranes, it cannot do so when it forms part of full-length Bax. It is nevertheless clear that some cautions should be taken in the extrapolation of results obtained with these peptides since there could not be, at least in some aspects, a simple correlation between the properties of the peptides and the function of the protein.

Since it has been demonstrated that the C-terminal part of Bax enhances the ability of this protein to destabilize membranes and it is simply involved in targeting Bax to mitochondria (*33*, *34*), this part may be involved in the formation of membrane pores by Bax, the existence of such pores having been suggested by a number of authors (*13*, *33*, *70*). It has been shown here that C-Bax is capable of spanning the membrane and hence of being perfectly capable of participating in forming such a pore.

In summary, we have shown that the C-terminal domain of Bax may become a membrane integral molecule, changing its conformation when it incorporates into the membrane, where its Trp residue remains near the lipid−water interface, and where it is capable of releasing carboxyfluorescein. The mutation S184K leads to some conformational changes in the peptide, which may still enter the membranes although it has a reduced capability to release carboxyfluorescein with the Trp residue supposedly close to C12. Finally, the deletion of S184 leads to a peptide with conformational changes with respect to the wild type, which, it is still able to penetrate the membrane and can induce very efficiently carboxyfluorescein release.

REFERENCES

1. Vaux, D. L., Haecker, G., and Strasser, A. (1994) *Cell 76*, 777−779.
2. Jacobson, M. D., Weil, M., and Raff, M. C. (1997) *Cell 88*, 347−354.
3. Green, D. R. (2000) *Cell 102*, 1−4.
4. Adams, J. M., and Cory, S. (1998) *Science 281*, 1322−1326.
5. Kelekar, A., and Thompson, C. B. (1998) *Trends Cell Biol. 8*, 324−330.
6. Kroemer, G. (1997) *Nat. Med. 3*, 614−620.
7. Reed, J. C. (1997) *Nature 387*, 773−776.
8. Chao, D. T., and Korsmeyer, S. T. (1998) *Annu. Rev. Immunol. 16*, 395−419.
9. Oltvai, Z. N., Milliman, C. L., and Korsmeyer, S. J. (1993) *Cell 74*, 609−619.
10. Kroemer, G. (1997) *Nat. Med. 3*, 614−620.
11. Lutz, R. J. (2000) *Biochem. Soc. Trans. 28*, 51−56.
12. Chittenden, T., Flemington, C., Houghton, A. B., Ebb, R. G., Gallo, G. J., Elangovan, B., Chinnadurai, G., and Lutz, R. J. (1995) *EMBO J. 14*, 5589−5596.
13. Jürgensmeier, J. M., Xie, Z., Deveraux, Q., Ellerby, L., Bredesen, D., and Reed, J. C. (1998) *Proc. Natl. Acad. Sci. U.S.A. 95*, 4997−5002.
14. Kluck, R. M., Bossy-Wetzel, E., Green, D. R., and Newmeyer, D. D. (1997) *Science 275*, 1132−1136.
15. Rossé, T., Olivier, R., Monney, L., Rager, M., Conus, S., Fellay, I., Jansen B., and Borner, C. (1998) *Nature 391*, 496−499.
16. Van der Heiden, M. G., Chandel, N. S., Williamson, E. K., Schumacker, P. T., and Thompson, C. B. (1997) *Cell 91*, 627−637.
17. Marzo, I., Brenner, C., Zamzami, N, Jurgensmeier, J. M., Susin, S. A., Vieira, H. L., Prevost, M. C., Xie, Z., Matsuyama, S. Reed, J. C., and Kroemer, G. (1998) *Science 281*, 2027−2031.
18. Narita, M., Shimizu, S., Ito, T., Chittenden, T., Lutz, R. J., Matsuda, H., and Tsujimoto, Y. (1998) *Proc. Natl. Acad. Sci. U.S.A. 95*, 14681−14686.
19. Shimizu, S., Narita, M., and Tsujimoto, Y. (1999) *Nature 399*, 483−487.
20. Brenner, C., Cadiou, H., Vieira, H. L., Zamzami, N., Marzo, I., Xie, Z., Leber, B., Andrews, D., Duclohier, H., Reed, J. C., and Kroemer, G. (2000) *Oncogene 19*, 329−336.
21. Susin, S. A., Lorenzo, H. K., Zamzami, N., Marzo, I., Snow, B. E., Brothers, G. M., Mangion, J., Jacotot, E., Costantini, P., Loeffler, M., Larochette, N., Goodlett, D. R., Aebersold, R., Siderovski, D. P., Penninger, J. M., and Kroemer, G. (1999) *Nature 397*, 441−446.
22. Liu, X., Kim, C. N., Yang, J., Jemmerson, R., and Wang, X. (1996) *Cell 86*, 147−157.
23. Antonsson, B., Conti, F., Ciavatta, A. M, Montessuit, S., Lewis, S., Martinou, I., Bernasconi, L., Bernard, A., Mermod, J. J., Mazzei, G., Maundrell, K., Gambale, F., Sadoul, R., and Martinou, J. C. (1997) *Science 277*, 370−372.
24. Schendel, S. L., Xie, Z., Montal, M. O., Matsuyama, S., Montal, M., and Reed, J. C. (1997) *Proc. Natl. Acad. Sci. U.S.A. 94*, 5113−5118.
25. Minn, A. J., Vélez, P., Schendel, S. L., Liang, H., Muchmore, S. W., Fesik, S. W., Fill, M., and Thompson, C. B. (1997) *Nature 385*, 353−357.
26. Schlesinger, P. H., Gross, A., Yin, X. M., Yamamoto, K., Saito, M., Waksman, G., and Korsmeyer, S. J. (1997) *Proc. Natl. Acad. Sci. U.S.A. 94*, 11357−113632.
27. Wolter, K. G., Hsu, Y. T., Smith, C. L., Nechushtan, A., Xi, X. G., and Youle, R. J. (1997) *J. Cell Biol. 139*, 1281−1292.
28. Gross, A., Jockel, J., Wei, M. C., and Korsmeyer, S. J. (1998) *EMBO J. 17*, 3878−3885.
29. Goping, I. S., Gross, A., Lavoie, J. N., Nguyen, M., Jemmerson, R., Roth, K., Korsmeyer, S. J., and Shore, G. C. (1998) *J. Cell. Biol. 143*, 207−215.
30. Antonsson, B., Montessuit, S., Sanchez. B., and Martinou, J. C. (2001) *J. Biol. Chem. 276*, 11615−11623.
31. Suzuki, M., Youle, R. J., and Tjandra, N. (2000) *Cell 103*, 645−654.
32. Gao, G., and Dou, Q. P. (2000) *J. Cell. Biochem. 80*, 53−72.
33. Basañez, G., Nechustan, A., Drozhinin, O., Chanturiya, A., Choe, E., Tutt, S., Wood, K. A., Hsu, Y. T., Zimmemberg, J., and Youle, R. J. (1999) *Proc. Natl. Acad. Sci. U.S.A. 96*, 5492−5497.
34. Oliver L, Priault M, Tremblais K, LeCabellec M, Meflah K, Manon S, Vallette FM. (2000) *FEBS Lett. 487*, 161−165.
35. Nechushtan, A., Smith, C. L., Hsu, Y. T, and Youle, R. J. (1999) *EMBO J. 18*, 2330−2341.
36. Quinn, P. J., and Chapman, D. (1980) *CRC Crit. Rev. Biochem. 8*, 1−117.
37. Arrondo, J. L. R., Muga, A., Castresana, J., Bernabeu, C., and Goñi, F. M. (1989) *FEBS Lett. 252*, 118−120.
38. Arrondo, J. L. R., Castresana, J., Valpuesta, J. M., and Goñi, F. M. (1994) *Biochemistry 33*, 11650−11655.
39. Lehrer, S. S., and Leavis, P. C. (1978) *Methods Enzymol. 49*, 222−236.
40. Weinstein, J. N., Yoshikami, S., Henkart, P., Blumenthal, R., and Hagins, W. A. (1977) *Science 195*, 489−492.
41. Rex, S. (1996) *Biophys. Chem. 58*, 75−85.
42. Rex, S., and Schwarz, G. (1998) *Biochemistry 37*, 2336−2345.
43. Simon, C. G., and Gear, A. R. L. (1998) *Biochemistry 37*, 2059−2069.
44. Hope, M. J., Bally, M. B., Webb, G., and Cullis, P. R. (1985) *Biochim. Biophys. Acta 812*, 55−65.
45. Lakowicz (1983) in *Principles of Fluorescence Spectroscopy*, pp 112−152, Plenum Press, New York and London.

46. Álvarez, J., Haris, P. I., Lee, D. C., and Chapman, D. (1987) *Biochim. Biophys. Acta 916*, 5−12.
47. Arrondo, J. L. R., Young, N. M., and Manstch, H. H. (1988) *Biochim. Biophys. Acta 952*, 261−268.
48. Muga, A., Arrondo, J. L., Bellon, T., Sancho, J., and Bernabeu, C. (1993) *Arch. Biochem. Biophys. 300*, 451−457.
49. Martínez-Senac, M. M., Corbalán-García, S., and Gómez-Fernández, J. C. (2000) *Biochemistry 39*, 7744−7752.
50. Arrondo, J. L. R., and Goñi, F. M. (1999) *Prog. Biophys. Mol. Biol. 72*, 367−405.
51. Jackson, M., Haris, P. I., and Chapman, D. (1991) *Biochemistry 30*, 9681−9686.
52. Haris, P. I., and Chapman, D. (1995) *Biopolymers 37*, 251−263.
53. Surewicz, W. K., Leddy, J. J., and Mantsch, H. H. (1990) *Biochemistry 29*, 8106−8111.
54. Fabian, H., Schultz, C., Naumann, D., Landt, O., Hahn, V., and Saenger, W. (1993) *J. Mol. Biol. 232*, 967−981.
55. Azuaga, A. I., Sepulcre, F., Padrós, E., and Mateo, P. L. (1996) *Biochemistry 35*, 16328−16335.
56. Chehin, R., Iloro, I., Marcos, M. J., Villar, E., Shnyrov, V. L., and Arrondo, J. L. R. (1999) *Biochemistry 38*, 1525−1530.
57. Arrondo, J. L. R., Muga, A., Castresana, J., and Goñi, F. M. (1993) *Prog. Biophys. Mol. Biol. 59*, 23−56.
58. Gómez-Fernández, J. C., Baena, M. D., Teruel, J. A., Villalaín, J., and Vidal, C. J. (1985) *J. Biol. Chem. 260*, 7168−7170.
59. Breukink, E., Van Kraaij, C., Van Dalen, A., Demel, R. A., Siezen, R. J., De Kruijff, B., and Kuipers, O. P. (1998) *Biochemistry 37*, 8153−8162.
60. Wang, S. X., Cai, G. P., and Sui, S. F. (1999) *Biochemistry 38*, 9477−9484.
61. Agirre, A., Flach, C., Goñi, F. M., Mendelsohn, R., Valpuesta, J. M., Wu, F., and Nieva, J. L. (2000) *Biochim. Biophys. Acta 1467*, 153−164.
62. Liu, R., Siemiarczuk, A., and Sharom, F. J. (2000) *Biochemistry 39*, 14927−14938.
63. Gómez-Fernández, J. C., Goñi, F. M., Bach, D., Restall, C. J., and Chapman, D. J. (1980) *Biochim. Biophys. Acta 598*, 502−516.
64. Hoffmann, W., Pink, D. A., Restall, C. J., and Chapman, D. (1981) *Eur. J. Biochem. 114*, 585−589.
65. Alonso, A., Restall, C. J., Turner, M., Gómez-Fernández, J. C., Goñi, F. M., and Chapman, D. (1982) *Biochim. Biophys. Acta 689*, 283−289.
66. Goñi, F. M., Cózar, M., Alonso, A., Durrani, A., García-Segura, L. M., Lee, D., Monreal, J., and Chapman, D. (1988) *Eur. J. Biochem. 174*, 641−646.
67. Azpiazu, I., Gómez-Fernández, J. C., and Chapman, D. (1993) *Biochemistry 32*, 10720−10726.
68. Soloaga, A., Veiga, M. P., García-Segura, L. M., Ostolaza, H., Brasseur, R., and Goñi, F. M. (1999) *Mol. Microbiol. 31*, 1013−1024.
69. Martínez-Senac, M. M., Corbalán-García, S., and Gómez-Fernández, J. C. (2001), unpublished results.
70. Nouraini, S., Six, E., Matsuyama, S., Krajewski, S., and Reed, J. C. (2000) *Mol. Cell. Biol. 20*, 1604−1615.

BI010667D